Toxicology Letters 257 (2016) 23–37

Contents lists available at ScienceDirect

Toxicology Letters

journal homepage: www.elsevier.com/locate/toxlet

# Pulmonary and pleural inflammation after intratracheal instillation of short single-walled and multi-walled carbon nanotubes

Katsuhide Fujita[a,b,*], Makiko Fukuda[b], Shigehisa Endoh[b], Junko Maru[b], Haruhisa Kato[b,c], Ayako Nakamura[c], Naohide Shinohara[a,b], Kanako Uchino[b], Kazumasa Honda[a,b]

[a] Research Institute of Science for Safety and Sustainability (RISS), National Institute of Advanced Industrial Science and Technology (AIST), Tsukuba, Ibaraki 305-8569, Japan
[b] Technology Research Association for Single Wall Carbon Nanotubes (TASC), Tsukuba, Ibaraki 305-8565, Japan,
[c] National Metrology Institute of Japan (NMIJ), National Institute of Advanced Industrial Science and Technology (AIST), Tsukuba, Ibaraki 305-8565, Japan

## HIGHLIGHTS

- Short SWCNTs induced persistent pulmonary inflammation over a 90-day period following instillation.
- Pulmonary inflammation after short MWCNT instillation decreased in a time-dependent manner.
- MWCNT instillation induced greater levels of pleural inflammation than did short SWCNTs.
- Short SWCNTs and MWCNTs underwent lymphatic drainage to the mediastinal lymph nodes after pleural penetration.
- The extent and time-dependent changes of pulmonary and pleural inflammation differed following SWCNT and MWCNT instillations.

## GRAPHICAL ABSTRACT

Hypothetical model of SWCNT- or MWCNT-induced pulmonary and pleural inflammation.

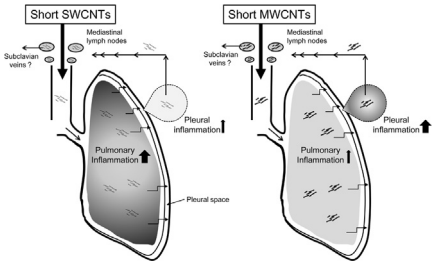


## ARTICLE INFO

*Article history:*
Received 12 February 2016
Received in revised form 20 May 2016
Accepted 28 May 2016
Available online 31 May 2016

*Keywords:*
Single-walled carbon nanotubes (SWCNTs)
Multi-walled carbon nanotubes (MWCNTs)
Intratracheal instillation
Pulmonary inflammation
Pleural inflammation

## ABSTRACT

Relationships between the physical properties of carbon nanotubes (CNTs) and their toxicities have been studied. However, little research has been conducted to investigate the pulmonary and pleural inflammation caused by short-fiber single-walled CNTs (SWCNTs) and multi-walled CNTs (MWCNTs). This study was performed to characterize differences in rat pulmonary and pleural inflammation caused by intratracheal instillation with doses of 0.15 or 1.5 mg/kg of either short-sized SWCNTs or MWCNTs. Data from bronchoalveolar lavage fluid analysis, histopathological findings, and transcriptional profiling of rat lungs obtained over a 90-day period indicated that short SWCNTs caused persistent pulmonary inflammation. In addition, the short MWCNTs markedly impacted alveoli immediately after instillation, with the levels of pulmonary inflammation following MWCNT instillation being reduced in a time-dependent manner. MWCNT instillation induced greater levels of pleural inflammation than did short SWCNTs. SWCNTs and MWCNTs translocated in mediastinal lymph nodes were observed, suggesting that SWCNTs and MWCNTs underwent lymphatic drainage to the mediastinal lymph nodes after pleural

* Corresponding author at: Research Institute of Science for Safety and Sustainability (RISS), National Institute of Advanced Industrial Science and Technology (AIST), Tsukuba, Ibaraki 305-8569, Japan.
*E-mail address:* ka-fujita@aist.go.jp (K. Fujita).

http://dx.doi.org/10.1016/j.toxlet.2016.05.025

penetration. Our results suggest that short SWCNTs and MWCNTs induced pulmonary and pleural inflammation and that they might be transported throughout the body after intratracheal instillation. The extent of changes in inflammation differed following SWCNT and MWCNT instillation in a time-dependent manner.


## 1. Introduction

Concerns regarding the influence of manufactured nanomaterials on human health have arisen concurrently with advances in nanotechnology. CNTs will potentially be used in a wide range of industrial products, and their potential toxicities has been vigorously debated. Safety assessment of CNTs during the initial research and development stages will provide rational risk assessment and management in the workplace.

Several studies on the pulmonary toxicity of SWCNTs and MWCNTs using *in vivo* rodent models have also been reported (Warheit et al., 2004; Lam et al., 2004; Shvedova et al., 2014; Morimoto et al., 2012a,b; Fujita et al., 2015a; Ma-Hock et al., 2009; Pauluhn, 2010; Muller et al., 2005). However, it remains unclear how the physical properties of CNTs relate to pulmonary toxicity. The fiber-pathogenicity paradigm is characterized by robust structure/toxicity relationships that enable the prediction of fiber-related pathogenicity, depending on their length, thickness, and biopersistence (Donaldson et al., 2010). While it is debatable whether this paradigm is applicable to CNTs, the relationships between the physical properties of CNTs and their toxicities have been discussed (Donaldson et al., 2013). Poland et al. (2008) demonstrated that CNTs in the form of long fibers showed a similar, or greater, propensity to produce inflammation and fibrosis in the peritoneal cavity, compared to that produced by long asbestos fibers. If fibers exceed the maximal length that a macrophage can engulf (~15 μm), macrophages cannot remove them, resulting in 'frustrated' pro-inflammatory effects. Frustrated phagocytosis is accompanied by the release of oxidants and cytokines as well as lysosomal destabilization, increasing the recruitment of inflammatory cells to the lungs and activating the surrounding epithelial cells, in turn leading to an inflammatory response (Donaldson et al., 2013). Long fibers can be defined as fibers that significantly exceed the size of macrophages and are usually considered 10–20 mm long (Donaldson et al., 2006).

In contrast, neither short asbestos fibers nor short, tangled CNTs caused significant inflammation (Poland et al., 2008). Short fibers might be effectively phagocytosed and cleared by macrophages (Donaldson et al., 2013). A smaller-sized MWCNT induced stronger inflammation and higher 8-hydroxydeoxyguanosine levels in lung tissue than did a larger-sized, needle-like type of MWCNT (Xu et al., 2014). Other researchers showed that short MWCNTs (length = 1–5 μm, diameter = 14.84 nm) had stronger potential for inducing the accumulation of polymorphonuclear cells, whereas long MWCNTs (length = 13 μm, diameter = 84.89 nm) increased interleukin-6 levels in BALFs. Alveolar septal fibrosis was only observed with short MWCNTs. Type II pneumocyte hypertrophy was only detected with long MWCNTs (Mühlfeld et al., 2012).

Furthermore, only limited research has been conducted to investigate pulmonary inflammation caused by short-fiber SWCNTs. Previously, we used a rat intratracheal instillation test to elucidate the effect of SWCNT size on pulmonary toxicity (Fujita et al., 2015b). SWCNTs formed as relatively thin bundles with short linear shapes (approximate 0.5 μm in length), which elicited delayed pulmonary inflammation with slower recovery. In contrast, SWCNTs with relatively thicker bundles and longer linear shapes (approximate 1.6 μm in length) sensitively induced responses in alveolar macrophages and elicited acute lung inflammation shortly after inhalation. We hypothesized that these responses are associated with bundle sizes and that short SWCNTs cause significant pulmonary inflammation.

In addition, the translocation of CNTs through the lungs to the pleural space after exposure is key for distinguishing their effects on human health. Evidence suggests that MWCNTs reach the pleura in mice or rats after a single inhalation exposure (Ryman-Rasmussen et al., 2009; Porter et al., 2013; Xu et al., 2012). Long MWCNT fibers in the lung and their retention in the parietal pleura can lead to the initiation of inflammation and pleural pathology, such as mesothelioma (Donaldson et al., 2010). If pleural penetration results in adverse health outcomes, extensive investigation is needed to fully assess this issue (Porter et al., 2010). A longer-sized, needle-like type of MWCNT (length = 8 μm, diameter = 150 nm) induced stronger inflammatory reactions, including increased inflammatory cell numbers and cytokine/chemokine levels in the pleural cavity lavage than did a smaller-sized MWCNT (length = 3 μm, diameter = 15 nm) (Xu et al., 2014). However, to our knowledge, no research has been conducted to study pleural inflammation after SWCNT exposure.

The aim of this study was to characterize differences in pulmonary and pleural inflammation with short-sized SWCNTs and MWCNTs after intratracheal instillation. We prepared short SWCNT and MWCNT suspensions and conducted *in vivo* intratracheal-instillation tests in rats. Total protein and cytokine analysis, cell counts in BALFs, histopathological examinations, and comprehensive gene-expression microarray analysis were performed on dissected lungs over a 90-day period following the instillations. SWCNT and MWCNT translocation to the mediastinal lymph nodes were investigated by a transmission electron microscopy (TEM) analysis.

## 2. Materials and method

### 2.1. Test materials and their preparation

Bulk SWCNTs were obtained from the Technology Research Association for Single-Wall Carbon Nanotubes (Japan). The Fe content was measured by inductively coupled plasma mass spectrometry (ICP-MS; ELEMENT XR™, Thermo Fisher Scientific Inc., Waltham, MA, US). A G/D ratio (intensity ratio of the G and D bands in Raman scattering) of 85 for the SWCNTs was determined using a DXR Raman spectrometer (Thermo Fisher Scientific Inc.). Bulk MWCNTs (MWNT-7) were purchased from Mitsui & Co., Ltd. (Tokyo, Japan). A carbon content of 99.79%, a Brunauer–Emmett–Teller-specific surface area of 23.0 $m^2$/g, and a G/D ratio of 11.0 were determined, as was described previously (Kobayashi et al., 2010). Bulk SWCNTs and MWCNTs were dispersed in stock suspensions at an estimated concentration of 1.0 mg/mL, as we described previously (Fujita et al., 2014). SWCNTs were dispersed into 10 mg/mL bovine serum albumin (BSA) dissolved in UltraPure™ DNase/RNase-Free Distilled Water (Thermo Fisher Scientific Inc.) for 4 h, using an ultrasonic homogenizer. SWCNTs were centrifuged, and the resulting supernatant was filtered through a cell strainer with a 40-μm nylon mesh for removing large CNT agglomerates (Becton, Dickinson & Company, Franklin Lakes, NJ, US). The filtrates were used as SWCNT stock suspensions. MWCNTs were dispersed into a 10 mg/mL BSA dissolved in UltraPure™

DNase/RNase-Free Distilled Water (Thermo Fisher Scientific Inc.) for 1.5 h using an ultrasonic bath, and the resulting supernatant was filtered through a cell strainer with a 40-μm nylon mesh to remove large CNT agglomerates (Becton, Dickinson & Company). The filtrates were used as MWCNT stock suspensions. No endotoxin in the SWCNT and MWCNT stock suspensions was detected using the *Limulus* Amebocyte Lysate test (Associates of Cape Cod, Inc., MA, USA; data not shown).

### 2.2. Characterization of SWCNTs or MWCNTs in working solutions

SWCNT and MWCNT stock suspensions and 10-fold dilutions in phosphate-buffered saline (PBS) were used in rat intratracheal-instillation tests as working solutions. We denoted the former working solutions as SW-H or MW-H, and the latter working solutions as SW-L or MW-L, respectively, to reflect their relatively high and low CNT concentrations. The concentrations of SWCNTs or MWCNTs in working solutions were determined by measuring their UV–vis absorption spectra with a JASCO V7200DS spectrometer (JASCO Corporation, Tokyo, Japan) at wavelengths ranging between 600 and 900 nm (Fujita et al., 2014). The zeta potentials of SWCNTs or MWCNTs dispersed in working solutions were measured using an ELS-Z Zeta-potential & Particle Size Analyzer (Otsuka Electronics Co.). The G/D Raman ratio was determined using a DXR Raman Microscope recorded with a 532-nm laser line (Thermo Fisher Scientific Inc., Waltham, MA, USA). The average particle size was determined using a Zetasizer Nano ZS system (Malvern Instruments, Ltd., UK). The lengths of SWCNTs or MWCNTs in working solutions were measured by TEM-based observations of 1000 SWCNT or MWCNTs bundles. The diameters of SWCNTs or MWCNTs in working solutions were measured by Raman spectroscopy or TEM-based observations, respectively.

### 2.3. Animals and experimental design

Nine-week-old male Wistar rats purchased from Japan SLC, Inc. (Shizuoka, Japan) were stratified into 3 groups (n = 9 per group per time point). The average rat body weight before instillation treatment was approximately 220 g. Rats were anesthetized with isoflurane (Mylan Inc., Tokyo, Japan) and intratracheally administered with 0.4 mL of 10-fold diluted working solutions (SW-L or MW-L, approximately 0.15 mg/kg) or undiluted working solutions (SW-H or MW-H, approximately 1.5 mg/kg) in a single injection, using an aerosolizing microsprayer (MicroSprayer® IA-1B, Penn-Century, Wyndmoor, PA, USA). We ensured that the tip of the microsprayer was carefully positioned in the trachea near to, but not touching the carina for appropriate intratracheal instillation. The vehicle control group was administered 0.4 mL of 10 mg/mL BSA solution/rat. Assuming that the average daily exposure time is 8 h/day, 5 days/week for workers in a working environment, we calculated that an instillation exposure of 1.5 mg/kg CNTs corresponds to pulmonary deposition amounts of 240–2000 days (8 month-5.5 years) in a working environment (Kobayashi et al., 2010). After intratracheal instillation treatment, rats were housed within polycarbonate cages at a controlled temperature of 23 °C and fed a chow diet *ad libitum*. After the instillations, the viabilities and general conditions of rats were observed once a day until they were sacrificed. The body weight of each rat was measured before instillation and at 1, 3, 7, 30, and 90 days post-instillation exposure. Morphological observations, BALF analysis, pleural cavity lavage fluid (PCLF) analysis, histopathological examination, and comprehensive gene-expression microarray analysis were performed on dissected lungs at 1, 3, 7, 30, and 90 days post-instillation exposure. All procedures and animal handling were approved by the Institutional Animal Care and Use Committee of Technology Research Association for Single Wall Carbon Nanotubes, the National Institute of Advanced Industrial Science and Technology, and the Public Interest Incorporated Foundation at the BioSafety Research Center (Shizuoka, Japan). Instillation with SWCNTs and MWCNTs used in this study was performed at several weeks post-instillation with vehicle control and the SWCNTs used in our previous study (Fujita et al., 2015b). The present study used vehicle control data for cell counts, MIP-1α levels in BALFs, and gene-expression profiles for reduction of animal use.

### 2.4. Cell counts, total protein, and cytokine assays with BALFs

Rats were anesthetized with isoflurane (Mylan, Inc.) and euthanized by exsanguination. The left bronchus was clamped with forceps, and the right bronchus was cannulated. Subsequently, 3 mL of heated (37 °C) saline (Otsuka Pharmaceutical Factory, Inc., Tokushima, Japan) was filled and aspirated to and from the right lungs to recover BALF fractions. This procedure was repeated 3 times. Supernatants were obtained by centrifuging BALFs at 250*g* for 10 min and were used for total protein and cytokine measurements. Centrifuged pellets were suspended in PBS and used to determine cell counts in BALF samples. The total number of cells in BALFs was counted using a hematology system (ADVIA120, Siemens Healthcare diagnostics, Inc., Tokyo, Japan). The total number of nucleated cells, macrophages, neutrophils, and lymphocytes were counted by May–Grünwald–Giemsa staining. Total protein concentrations in BALFs were measured with an automatic biochemical analyzer (7170, Hitachi High-Tech Fielding Corporation, Tokyo, Japan). The levels of macrophage inflammatory protein-1 alpha (MIP-1α), macrophage chemoattractant protein-1 (MCP-1), interleukin-1 alpha (IL-1α), interleukin-1 beta (IL-1β), tumor necrosis factor alpha (TNF-α), growth-related oncogene (GRO/KC), interleukin-18 (IL-18), and secreted phosphoprotein 1 (SPP1, also known as osteopontin) were measured using a MILLIPLEX® MAP Rat Cytokine/Chemokine Magnetic Bead Panel and a Luminex 200 System (Merck Millipore, Billerica, MA, US).

### 2.5. Histopathological analysis

After rats were sacrificed, their left lungs were filled with 4% buffered paraformaldehyde prior to processing for histopathological examinations. Fixed left lung tissues were embedded in paraffin, and stained with hematoxylin and eosin. Digital images of each lung section were obtained for the alveoli, alveolar walls, bronchioles, and vessels for histopathological evaluation. The average pulmonary–histopathology scores given to individual animals were calculated from a complete pathological examination, and are reported here as follows: 0, not remarkable; 1, slight; 2, moderate; and 3, marked; based upon the relative evaluation of histopathological findings.

### 2.6. Cell counts, total protein, and cytokine assays with PCLFs

PCLFs were collected from euthanized rats by exsanguination. Small, surgical incisions were made in the diaphragm, after which a polystyrene tube with an attached syringe was inserted into the pleural cavity. The pleural cavity was washed gently with 5 mL of heated (37 °C) PBS. Supernatants were obtained by centrifuging PCLFs at 800*g* for 10 min at 4 °C and were used for total protein and cytokine measurements. Total protein concentrations in PCLFs were measured with an automatic biochemical analyzer (Hitachi High-Tech Fielding Corporation). The levels of MIP-1α, MCP-1, IL-1α, IL-1β, TNF-α, GRO/KC, IL-18, and SPP1 were measured using a MILLIPLEX® MAP Rat Cytokine/Chemokine Magnetic Bead Panel and a Luminex 200 System (Merck Millipore). Centrifuged pellets

were suspended in PBS and used to determine cell counts in PCLF samples. The total numbers of cells in PCLFs was counted using a hematology system (ADVIA120). The number of total nucleated cells, macrophages, neutrophils, and lymphocytes were counted by May–Grünwald–Giemsa staining.

### 2.7. TEM observations

Mediastinal lymph nodes in rats intratracheally instilled with SW-H or MW-H, were fixed using 2.5% (v/v) glutaraldehyde for 2 h at 4 °C and 1% osmium oxide solution for 2 h at 4 °C, dehydrated in ethanol, and embedded in a commercially available epoxy resin

A

| Sample | Concentration of CNTs (mg/mL) | G/D ratio | Fe (μg/mL) | Particle size (nm) | Length* (μm) | Tube diameter (nm) |
|---|---|---|---|---|---|---|
| SW-L | 0.08 | NT | NT | NT | NT | 1.7-2.1 |
| SW-H | 0.81 | 10.7 | 49 | 557.0 | 0.50 | NT |
| MW-L | 0.08 | NT | NT | NT | NT | 60-100 |
| MW-H | 0.84 | 8.8 | 3.9 | 622.0 | 1.81 | NT |

*Values are expressed as arithmetic mean. NT: not tested.

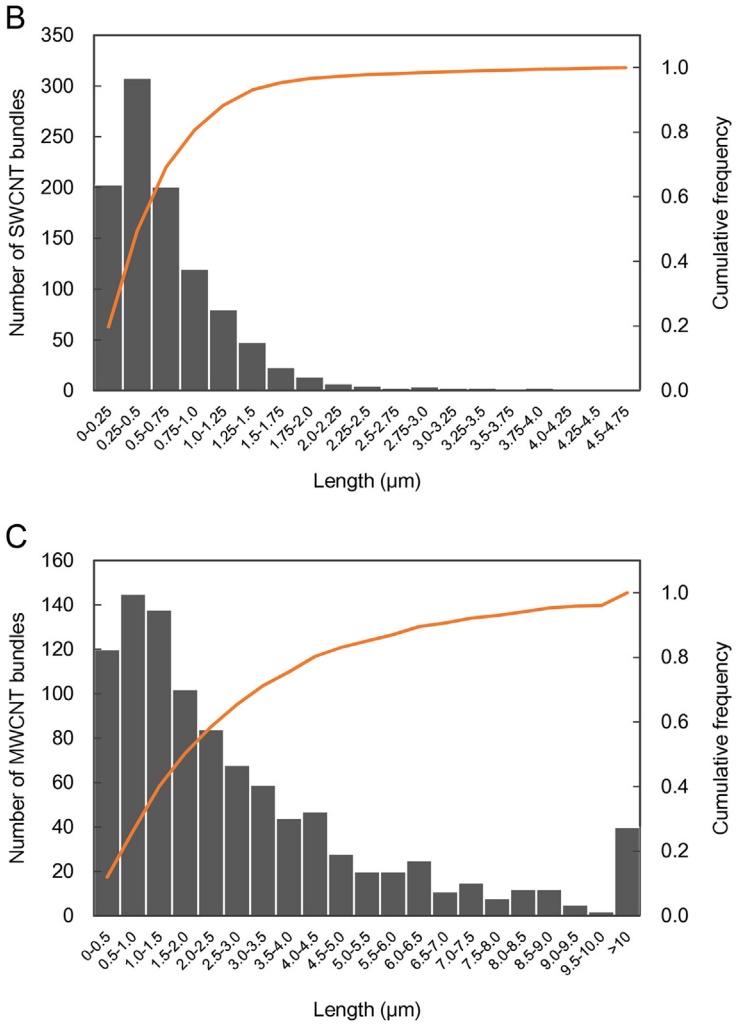


**Fig. 1.** Characterization of SWCNTs and MWCNTs dispersed in working solutions for rat intratracheal instillation tests (A). TEM images of SWCNTs in SW-H (B and C) and MWCNTs in MW-H (D and E). High-magnification micrographs (C and E). Distribution of SWCNT (F) and MWCNT (G) lengths in working solutions, as evaluated in digital TEM images.

(TAAB Laboratories Equipment Ltd., Reading, England). Samples were transferred to fresh resin in capsules and polymerized at 60 °C for 48 h. A TEM system at 75 kV (H-7000; Hitachi, Japan) was used to observe the intracellular distribution of SWCNTs or MWCNTs in the mediastinal lymph nodes of rats.

### 2.8. RNA extraction and DNA microarray experiments

Right lungs (n = 4 per group per time point) were homogenized using the QIAzol Lysis Reagent and a TissueRuptor (Qiagen; Tokyo, Japan). Total RNA from homogenates was extracted using the RNeasy Midi Kit (Qiagen), following the manufacturer's instructions. RNA was quantified using a NanoDrop 2000 spectrophotometer (Thermo Fisher Scientific Inc.; Waltham, MA, USA), and sample qualities were monitored with an Agilent 2100 Bioanalyzer (Agilent Technologies; Santa Clara, CA, USA). Cyanine-3-labeled complementary RNA (cRNA) was prepared from RNA using the One-Color Low RNA Input Linear Amplification PLUS Kit (Agilent Technologies), according to the manufacturer's instructions, followed by RNeasy column purification (Qiagen). Each labeled cRNA probe was used separately for hybridization to a $4 \times 44$ K Whole Rat Genome Microarray Kit (G4131F; Agilent Technologies), and hybridization was performed at 65 °C for 17 h. Hybridized microarray slides were washed according to the manufacturer's instructions and scanned with an Agilent DNA Microarray Scanner (G2565BA; Agilent Technologies) at 5-micron resolution. The scanned images were analyzed numerically using Agilent Feature Extraction Software, version 10.7.3.1 (Agilent Technologies).

### 2.9. Microarray data analysis

Normalized data were analyzed using GeneSpring GX software, version 11.5.1 (Agilent Technologies). Log fold-changes represent the ratio of the normalized intensity values of SW-H or MW-H-exposed samples to the normalized intensity value of vehicle control samples. Genes displaying log fold-change values $> 1$ were considered upregulated genes, whereas those displaying values $< -1$ were considered downregulated genes. Gene

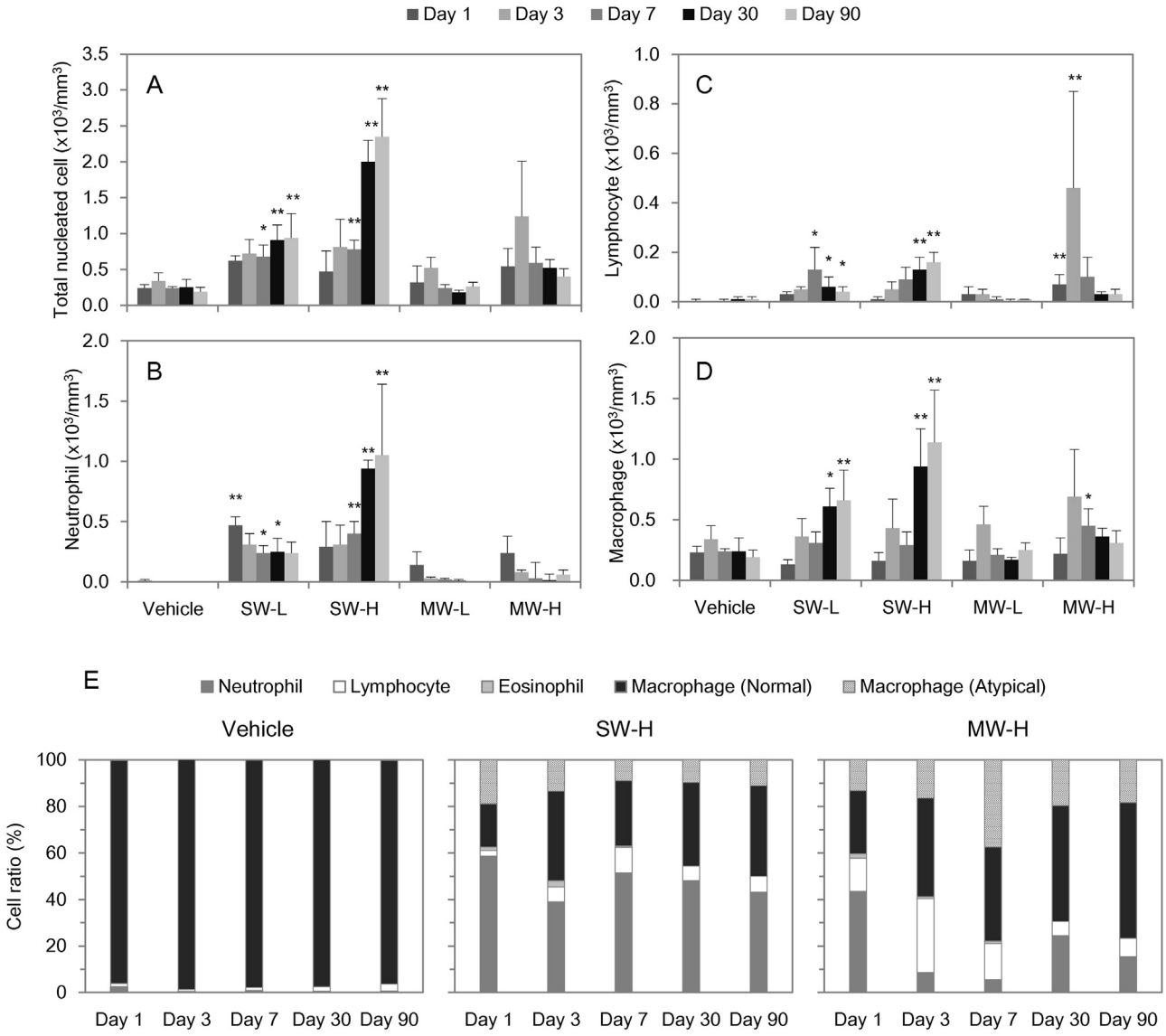


**Fig. 2.** Total nucleated cells (A), neutrophils (B), lymphocytes (C), and macrophages (D) in BALFs following exposure of rats to vehicle controls, SWCNTs (SW-L or SW-H), or MWCNTs (MW-L or MW-H) at the indicated time points. The resulting values were analyzed by comparing data from the treated and vehicle control groups by Dunnett's procedure based on the re-sampling method ($^{*}p < 0.05$, $^{**}p < 0.01$), after the data were found to be non-homogeneous by Bartlett's test for homogeneity of distribution ($p < 0.20$).

expression data for each experimental group were deposited into the Gene Expression Omnibus database (Accession number GSE75148; http://www.ncbi.nlm.nih.gov/projects/geo/). The web-based application GOstat (http://gostat.wehi.edu.au/) was used to identify statistically overrepresented Gene Ontology (GO) terms (Beissbarth and Speed, 2004) with the Rat Genome Database (RGD: http://rgd.mcw.edu/). Differences between control and experimental groups were evaluated using the Welch's unequal variance *t* test, which is suitable regardless of whether 2 groups have a similar or dissimilar variance. $p$ values $< 0.05$ were considered statistically significant.

### 2.10. Statistical analysis

All numerical values are represented as the mean ± SD. The resulting values were analyzed by comparing data from the treated groups to data from the vehicle control group by Dunnett's procedure, based on the re-sampling method ($^{*}p < 0.05$, $^{**}p < 0.01$), after the data were found to be non-homogeneous by Bartlett's test for homogeneity of distribution ($p < 0.20$).

## 3. Results

### 3.1. Characterization of CNTs dispersed in working solutions

Analysis with an absorption spectrometer demonstrated nearly equivalent CNT concentrations in the adjusted SWCNTs or MWCNT stock suspensions (Fig. 1A). Consequently, SWCNTs or MWCNTs in low-dose form (SW-L or MW-L) were administered to rats at approximately 0.15 mg/kg, and SWCNTs or MWCNTs in high-dose form (SW-H or MW-H) were administered to rats at approximately 1.5 mg/kg. The negative zeta potentials of all adjusted samples revealed that SWCNT or MWCNT particles were dispersed in working solutions. Raman spectrophotometric analysis revealed that the G/D ratio for bulk SWCNTs or MWCNTs decreased from 84.4 to 10.7 for SW-H, or from 14.2 to 8.8, respectively, for MW-H. The Fe contents in SW-H and MW-H were 49 μg/mL and 3.9 μg/mL, respectively. ICP-MS results revealed that the metal content (e.g., Y and Ni) of SW-H or MW-H was at an undetectable level. TEM images of representative SWCNT or MWCNT dispersions showed different morphological features in working solutions (data not shown). SWCNTs were observed to contain relatively thick SWCNT structures with a short linear shape. MWCNTs assembled into relatively thick bundles of MWCNTs, and a long linear shape with MW-H. Noticeably aggregated forms of SWCNTs in each working solution were not identified. The arithmetic mean lengths of the SWCNTs or MWCNTs were 0.50 μm (range, 0.05–8.14 μm) and 1.81 μm (range, 0.12–21.5 μm), respectively (Fig. 1B and C). We were unable to prepare longer SWCNTs owing to technical limitations. If we had been able to prepare longer SWCNTs and compare them with the MWCNTs (1.81 μm) used in our previous studies (Fujita et al., 2015b), we could have studied whether differences in length preferentially affected pulmonary inflammation more so than differences in composition.

### 3.2. General conditions

No clinical signs, such as abnormal behavior and irregular respiration, were observed during the observation period in any of the groups. One rat died each in the SW-L and MW-H groups immediately following intratracheal instillation.

### 3.3. BALF analysis

Lungs of anesthetized rats were excised and subjected to BALF analysis at 1, 3, 7, 30, and 90 days post-instillation exposure. The total nucleated cell, neutrophil, lymphocyte, and macrophage counts in BALFs from the SWCNT-exposed group significantly increased during the observation period (Figs. 2A–D). The results indicated that the relative proportion of neutrophils among the total nucleated cells increased in the SW-H-exposed group compared to that observed in the vehicle control groups (Fig. 2E). In MW-H-exposed group, high counts of total nucleated cells, neutrophils, and lymphocytes in BALFs were observed at 3 days post-instillation exposure, after which these counts decreased (Figs. 2A–D). These results indicated that both groups differed with respect to the relative proportion of neutrophils and normal and atypical macrophages (i.e., macrophage with phagocytized CNTs) among the total nucleated cells at 3 days post-instillation exposure. Furthermore, no dramatically higher counts

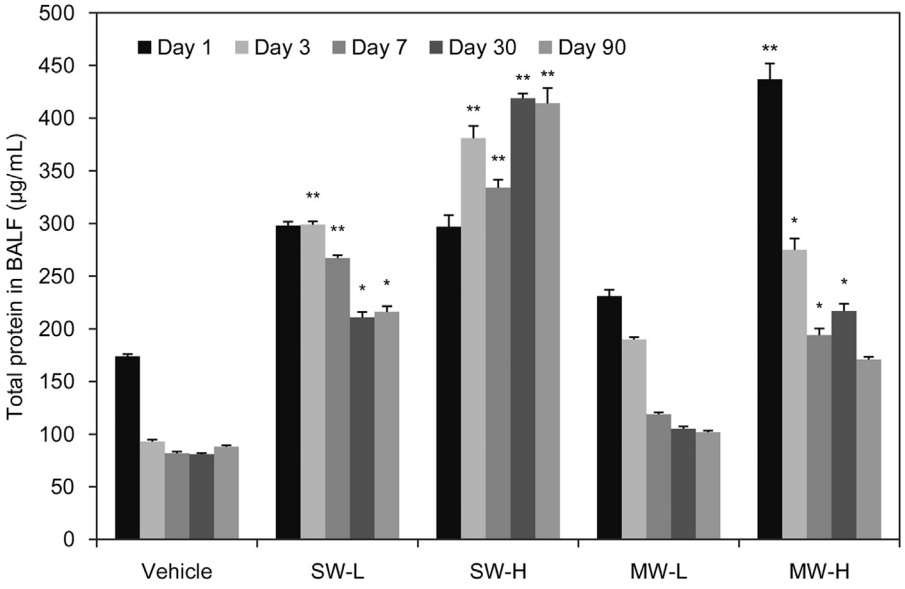


**Fig. 3.** Total protein content in BALFs following exposure of rats to vehicle controls, SWCNTs (SW-L or SW-H) or MWCNTs (MW-L or MW-H) at the indicated time points. The resulting values were analyzed by comparing data from the treated and vehicle control groups by Dunnett's procedure based on the re-sampling method ($^{*}p < 0.05$, $^{**}p < 0.01$), after the data were found to be non-homogeneous by Bartlett's test for homogeneity of distribution ($p < 0.20$).

of total nucleated cells or neutrophils were observed (Fig. 2E). Total protein levels in the SW-H group increased at 1 day post-instillation exposure and further significantly increased over time ($p < 0.01$). In contrast, the high total protein levels observed at 1 day post-instillation exposure ($p < 0.01$) decreased over time in the MW-H group (Fig. 3). MIP-1α, MCP-1, IL-18, and SPP1 levels in the SW-H group significantly increased, compared to those levels observed in the vehicle control groups during the observation period (Fig. 4). It was noted that the levels at 30 days and 90 days post-instillation exposure were remarkably high. MIP-1α, MCP-1, and SPP1 levels in the MW-H groups were significantly higher than those of vehicle control groups at 1 day post-instillation exposure. SPP1 induction increased in a time-dependent manner. No significant differences were found in the IL-1α, IL-1β, TNF-α, or

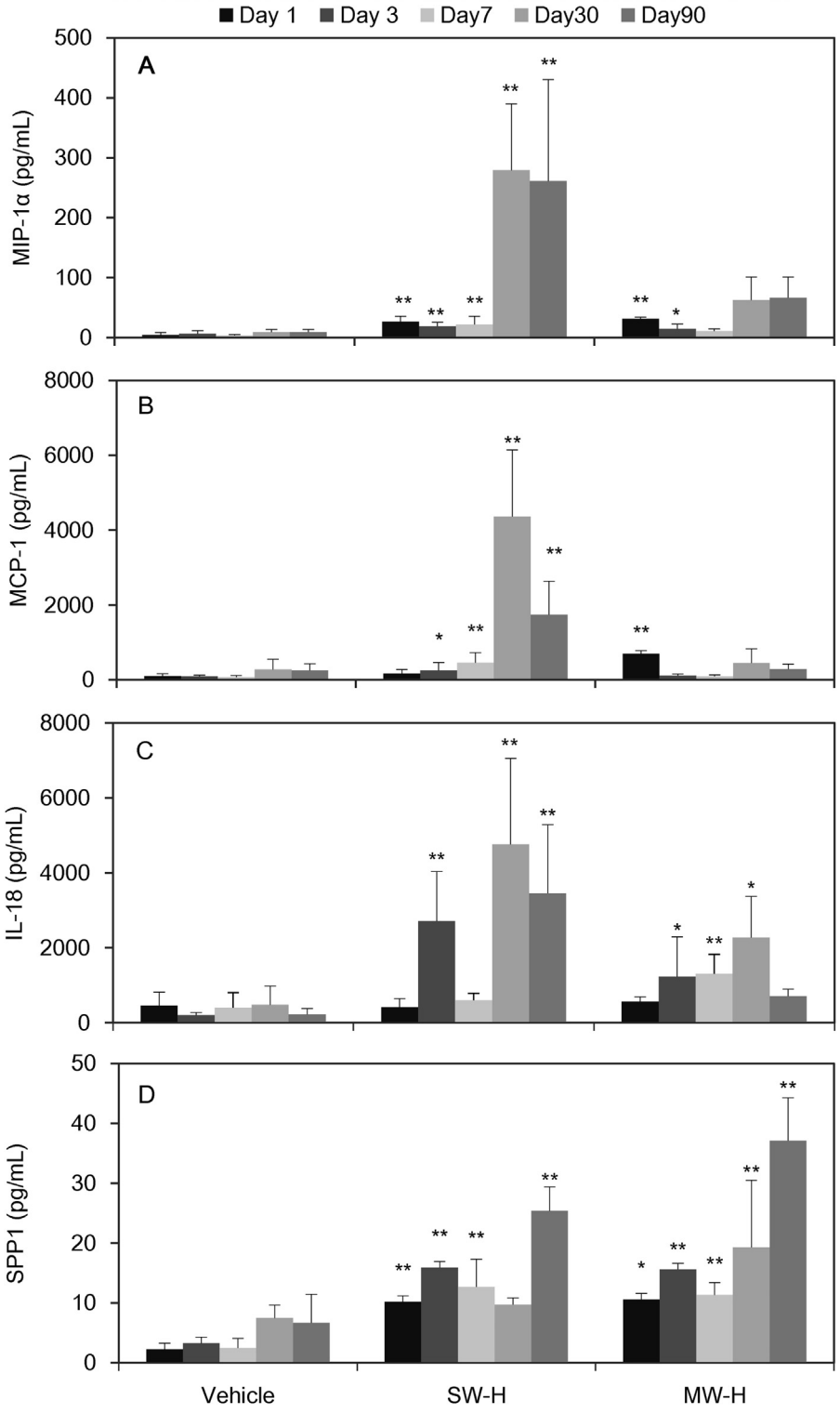


**Fig. 4.** The levels of MIP-1α (A), MCP-1 (B), IL-18 (C), and SPP1 (D) in BALFs following exposure of rats to vehicle controls, SWCNTs (SW-H), or MWCNTs (MW-H) at each time point. The resulting values were analyzed by comparing data from the treated and vehicle control groups by Dunnett's procedure based on the re-sampling method ($^{*}p < 0.05$, $^{**}p < 0.01$), after the data were found to be non-homogeneous by Bartlett's test for homogeneity of distribution ($p < 0.20$).

GRO/KC levels in either the SW-H or MW-H group (data not shown).

### 3.4. Pathological examination of lung tissues

Observations of gross pathology showed that SWCNT and MWCNT aggregates in dissected lungs and tracheas were incompletely eliminated at 90 days post-instillation exposure. The average pulmonary–histopathology severity scores for focal inflammatory changes (alveolitis), infiltration of neutrophils into the alveolus, infiltration of eosinophils into perivascular interstitial spaces, macrophage increases, and macrophage test-substance engulfment in the MW-H group were higher than those in the SW-H group at 1 and 3 days post-instillation exposure (Fig. 5A–D and Table 1). However, these scores time-dependently decreased at 7 days post-instillation exposure. The scores for infiltration of neutrophils into the alveolus, macrophage increases, and macrophage test-substance engulfment in the SW-H group were higher than those of the MW-H group at 7, 30, and 90 days post-instillation exposure (Fig. 5E–J and Table 1). Time-dependent increases in macrophage counts, macrophage test-substance engulfment, and foamy macrophages were observed in the SW-H groups. The scores given at 30 and 90 days post-instillation exposure were noticeably high (Table 1). Macrophage-containing

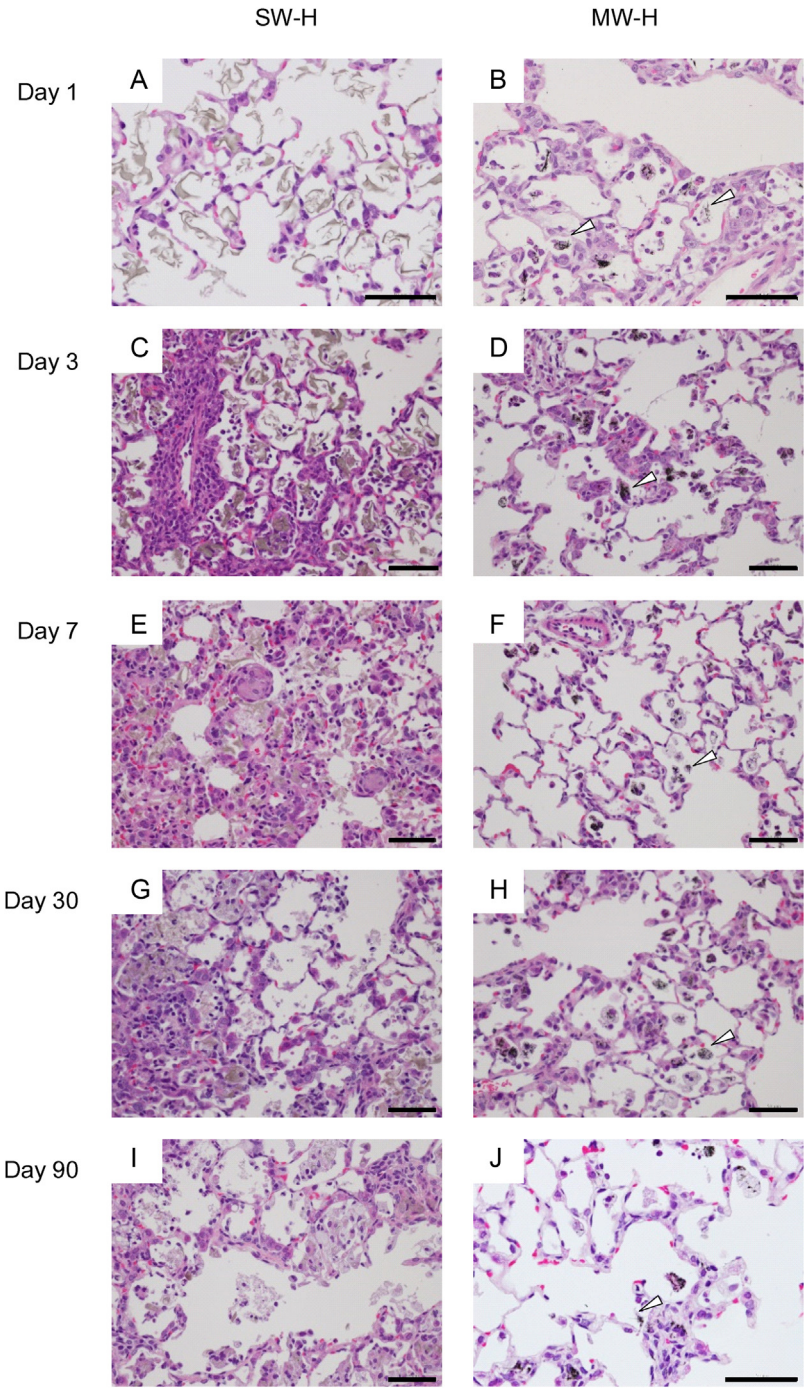


**Fig. 5.** Anatomical observations after instillation with SWCNTs or MWCNT. Lungs were dissected at 1, 3, 7, 30, or 90 days post-instillation exposure in groups of rats exposed to the vehicle control or a high dose of SWCNTs or MWCNTs (SW-H or MW-H). Micrographs of lung tissues from rats exposed to SWCNTs (A, C, E, G, and I) or MWCNTs (B, D, F, H, and J) at a high-dose. Arrows indicate MWCNTs protruding from alveolar walls and macrophages. Scale bar: 50 μm.

**Table 1**
Pulmonary–histopathology severity scores of rats exposed to vehicle controls, SW-L, SW-H, MW-L, or MW-H.

| Findings | Time point | Vehicle control group | Exposed group | | | |
|---|---|---|---|---|---|---|
| | | | SW-L | SW-H | MW-L | MW-H |
| Focal inflammatory change (alveolitis) | Day 1 | 0 | 1.0 | 1.0 | 1.3 | 2.0 |
| | Day 3 | 0 | 1.0 | 1.0 | 1.0 | 2.0 |
| | Day 7 | 0 | 1.0 | 2.0 | 0 | 1.4 |
| | Day 30 | 0 | 1.4 | 2.0 | 0 | 1.6 |
| | Day 90 | 0 | 2.0 | 2.0 | 0 | 1.0 |
| Alveolar neutrophilic infiltration | Day 1 | 0 | 1.3 | 1.3 | 1.2 | 1.8 |
| | Day 3 | 0 | 1.0 | 1.0 | 2.0 | 1.8 |
| | Day 7 | 0 | 1.4 | 2.0 | 0 | 1.0 |
| | Day 30 | 0 | 2.0 | 2.2 | 0 | 1.0 |
| | Day 90 | 0 | 1.7 | 2.0 | 0 | 0 |
| Perivascular eosinophilic infiltration | Day 1 | 0 | 1.2 | 1.6 | 1.3 | 2.2 |
| | Day 3 | 0 | 1.2 | 1.8 | 1.3 | 1.8 |
| | Day 7 | 0 | 1.8 | 2.2 | 0 | 1.6 |
| | Day 30 | 0 | 0 | 0 | 0 | 0 |
| | Day 90 | 0 | 0 | 0 | 0 | 0 |
| Eosinophilic peribronchial infiltration | Day 1 | 0 | 1.3 | 1.2 | 1.3 | 1.4 |
| | Day 3 | 0 | 1.3 | 2.0 | 1.0 | 1.4 |
| | Day 7 | 0 | 1.2 | 2.0 | 0 | 2.0 |
| | Day 30 | 0 | 0 | 0 | 0 | 0 |
| | Day 90 | 0 | 0 | 0 | 0 | 0 |
| Increased macrophages | Day 1 | 0 | 1.0 | 1.0 | 1.0 | 1.6 |
| | Day 3 | 0 | 2.0 | 1.5 | 1.0 | 1.8 |
| | Day 7 | 0 | 1.8 | 2.2 | 0 | 2.0 |
| | Day 30 | 0 | 1.8 | 2.6 | 0 | 1.8 |
| | Day 90 | 0 | 2.0 | 3.0 | 1.0 | 1.8 |
| Macrophages engulfing test substances | Day 1 | 0 | 1.0 | 1.0 | 0 | 1.2 |
| | Day 3 | 0 | 1.0 | 1.0 | 1.0 | 1.8 |
| | Day 7 | 0 | 1.0 | 1.8 | 0 | 1.2 |
| | Day 30 | 0 | 1.0 | 2.0 | 0 | 1.8 |
| | Day 90 | 0 | 1.0 | 2.0 | 1.0 | 1.0 |
| Foamy macrophages | Day 1 | 0 | 0 | 0 | 0 | 0 |
| | Day 3 | 0 | 0 | 0 | 0 | 0 |
| | Day 7 | 0 | 1.0 | 1.0 | 0 | 1.0 |
| | Day 30 | 0 | 1.8 | 2.4 | 0 | 1.3 |
| | Day 90 | 0 | 2.0 | 2.8 | 0 | 1.0 |
| Granuloma | Day 1 | 0 | 0 | 0 | 0 | 0 |
| | Day 3 | 0 | 0 | 0 | 0 | 0 |
| | Day 7 | 0 | 0 | 1.0 | 0 | 0 |
| | Day 30 | 0 | 0 | 1.5 | 0 | 0 |
| | Day 90 | 0 | 0 | 0 | 0 | 0 |
| Alveolar cell debris | Day 1 | 0 | 0 | 0 | 0 | 0 |
| | Day 3 | 0 | 0 | 0 | 0 | 0 |
| | Day 7 | 0 | 0 | 0 | 0 | 0 |
| | Day 30 | 0 | 1.0 | 1.8 | 0 | 0 |
| | Day 90 | 0 | 1.0 | 2.4 | 0 | 0 |
| Alveolar hemorrhaging | Day 1 | 0 | 1.0 | 1.5 | 1.0 | 1.0 |
| | Day 3 | 0 | 0 | 0 | 0 | 1.0 |
| | Day 7 | 0 | 0 | 1.0 | 0 | 0 |
| | Day 30 | 0 | 0 | 1.0 | 0 | 0 |
| | Day 90 | 0 | 0 | 0 | 0 | 0 |

The average severity scores given to individual animals were calculated from a complete pathological examination and assigned as follows: 0, not remarkable; 1, slight; 2, moderate; and 3, marked; based upon the relative evaluation of histopathological findings.

granuloma formation neighboring the sites of SW-H aggregates was accumulated at 7 and 30 days post-instillation exposure (Fig. 5E and Table 1). Cell debris, presumably from disruptions caused by macrophages infiltrating the alveoli, was observed in the SW-H groups at 30 and 90 days post-instillation exposure (Fig. 5G and I). MWCNT penetration through the alveolar wall and macrophages were observed in the MW-H groups at all observation periods (Figs. 5B, D, F, H, and J). No obvious morphological changes were observed in the vehicle control group (data not shown).

### 3.5. Gene expression profiling of rat lungs

Comprehensive gene-expression profiles using a DNA microarray revealed time-dependent changes in gene expression after rat lungs were intratracheally instilled with a high dose of SW-H or MW-H. Microarray data from these experiments were deposited in the Gene Expression Omnibus database under Accession Number GSE75148. A large number of upregulated and downregulated genes with $p$ values $< 0.05$ involved in the inflammatory response in the high-dose SW-H or MW-H group was consistently observed throughout the observation period (Table 2). Statistical analysis revealed small $p$ values for the GO term "inflammatory response" [GO: 0006954] for SW-H or MW-H-affected genes during the observation period. Similarly, the "immune system process" [GO: 0002376] or "response to stimulus" [GO: 0050896] GO terms for the SW-H or MW-H-affected genes were overrepresented during the observation period (data not shown). These results suggested that SW-H and MW-H-affected genes were intimately related to inflammatory responses, immune system processes, and responses to stimuli during the observation period. However, the time-dependent expression patterns of individual representative genes involved in responses to stimuli were quite different between the SW-H and MW-H groups during the observation period (Fig. 6). The expression levels of the *Ccl2, Ccl7, Ccl9, Ccl12, Mmp7, Mmp12,* and *Spp1* genes increased during the observation period in the SW-H group, except at 30 days post-instillation exposure. An inverse trend was observed with the MW-H group. The *Ccl2, Ccl7, Ccl12, Mmp7,* and *Spp1* genes were markedly upregulated in the MW-H group at 1 or 3 days post-instillation exposure, and then these levels decreased over time, up to 90 days post-instillation exposure.

### 3.6. PCLF analysis

Macrophage counts in PCLFs from the SW-H-exposed group significantly increased at 90 days post-instillation exposure ($p < 0.05$); however, no significant difference was found in total nucleated cell, neutrophil, and lymphocyte counts in PCLFs from the SW-L and SW-H-exposed groups during the observation period (Fig. 7). In contrast, total nucleated cells and macrophage counts in PCLFs from the MW-L and MW-H-exposed groups significantly increased at 30 and 90 days post-instillation exposure ($p < 0.01$). High total protein levels were found at 90 days post-instillation exposure ($p < 0.01$) in the group exposed to MW-H (Fig. 8). No significant difference was observed in the IL-18 and SPP1 levels between the SW-H and vehicle control groups. In contrast, these levels were significantly higher than those of the vehicle control groups at 30 and 90 days post-instillation exposure in the MW-H group ($p < 0.01$). These results suggested that short SWCNT instillation induced low levels of pleural inflammation and that short MWCNT instillation time-dependently induced pleural inflammation. IL-1β levels in the groups exposed to SW-H and MW-H were significantly lower than those measured in the vehicle control groups during the observation period (data not shown). No significant difference was found in the MIP-1α, MCP-1, IL-1α, TNF-α, and GRO/KC levels in the SW-H and MW-H groups (data not shown).

### 3.7. Transition of CNTs toward to mediastinal lymph nodes

TEM analysis showed that SWCNT bundles and MWCNTs were present in mediastinal lymph nodes in the SW-H and MW-H groups at 90 d post-instillation exposure, respectively (Fig. 9). Some SWCNT bundles and MWCNTs similar to those shown in Fig. 1 were observed.

## 4. Discussion

To identify differences between short SWCNTs and MWCNTs in pulmonary and pleural inflammation after intratracheal instillation, we prepared short SWCNT and MWCNT suspensions and conducted *in vivo* intratracheal-instillation tests in rats. Observations of gross pathology showed some commonalities in the lungs between rats administered SWCNTs and MWCNTs instillations, such as red patches in the lungs and black, red, or gray-colored lymph nodes in each group. During histopathological examinations, infiltration of inflammatory cells into alveoli, focal inflammatory changes (alveolitis) representing fibrosis and thickening surrounding the alveolar walls, and increasing macrophages laden with SWCNTs or MWCNTs were found throughout the observation period. Foamy macrophages were observed at 7 days post-instillation exposure. The histopathological severity increased in a dose-dependent manner, and SWCNTs induced pathological changes more so than did MWCNTs. Overall, these results indicated that both short SWCNTs and MWCNTs, as foreign materials deposited in the alveoli, initiated inflammatory responses such as neutrophil infiltration.

However, different types of inflammatory responses appeared to be elicited by short SWCNTs and MWCNTs, based on results from BALF analysis, histopathological findings, and gene-expression profiling. These differences were reflected by altered cell counts, total protein contents, and cytokine levels in BALFs. The total numbers of nucleated cells, neutrophils, lymphocytes, and macrophages in BALFs increased time- and dose-dependently in the SWCNT-exposed group. We suggest that neutrophils and macrophages incrementally phagocytosed SWCNTs that accumulated in the alveoli, leading to pulmonary inflammation in a time-dependent manner. In the MW-H-exposed group, high counts of total nucleated cells, neutrophils, and lymphocytes in BALFs were observed at 3 days post-instillation exposure, and their counts decreased subsequently in a time-dependent manner. Total protein levels in the SW-H exposed group increased at 1 day post-instillation exposure and further significantly increased over time, while these levels in the MW-H group showed time- and dose-dependent decreases. MIP-1α, MCP-1, IL-18, and SPP1 levels in the SW-H group were significantly higher than those of the vehicle control groups during the observation period.

Second, histopathological findings revealed morphological differences resulting from SWCNT and MWCNT administration. Cell debris, presumably caused by degraded macrophages

**Table 2**
Total number of differentially expressed genes with $P$ values $< 0.05$ involved in the inflammatory response [GO: 0006954] in the SW-H or MW-H group.

| | | Day 1 | Day 3 | Day 7 | Day 30 | Day 90 |
|---|---|---|---|---|---|---|
| SW-H | Upregulated genes | 32 | 23 | 53 | 30 | 52 |
| | Downregulated genes | 17 | 16 | 3 | 1 | 9 |
| MW-H | Upregulated genes | 37 | 38 | 29 | 30 | 32 |
| | Downregulated genes | 19 | 9 | 2 | 2 | 18 |

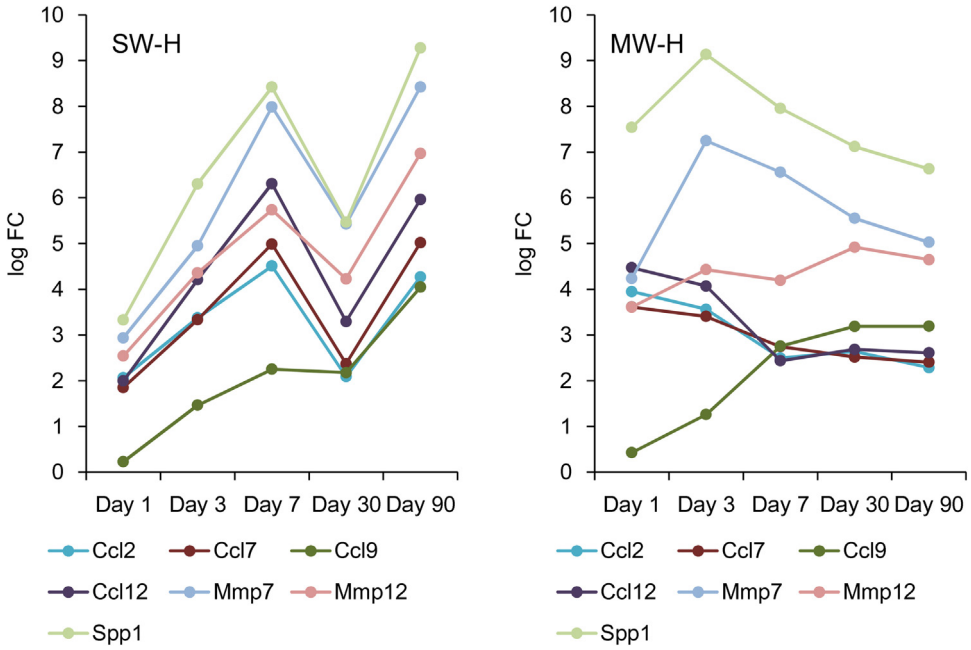


**Fig. 6.** Changes in the expression of genes involved in response to stimulus over time in rat lungs intratracheally instilled with SWCNTs or MWCNTs in the high-dose group. Numerical values represent log-fold gene expression changes relative to control levels.

infiltrating the alveoli, was observed at 30 and 90 days post-instillation exposure in the SWCNT-exposed group. Macrophage-containing granulomas surrounding sites of SWCNT aggregates accumulated at 7 and 30 days post-instillation exposure in the SW-H group. Alveolar macrophages appear to initiate SWCNT-induced pathogenesis through SWCNT phagocytosis, followed by the release of various cytokines that recruit distinct immune cells and promote granuloma formation (Chou et al., 2008). Our previous findings also showed that macrophage-containing granulomas develop around SWCNT-aggregation sites, which accumulated following instillation exposure (Fujita et al., 2015a, b). Granulomas can impair cellular and physiological lung functions, generating fibrosis, more defined nodules, and additional lesions (Lam et al., 2004). It is thought that granuloma formation around activated macrophages may protect surrounding host tissues from destructive chronic inflammation. However, the present study showed that macrophage-containing granulomas neighboring MWCNT-aggregation sites and cell debris were not present during the observation period. Kobayashi et al. reported that deposition of MWCNTs and the accumulation of macrophage, part of which were granulomatous, was observed in the alveoli and interstitium from 3 to 30 days post-exposure in the group exposed to 1 mg/kg MWCNTs (Kobayashi et al., 2010). The discrepancies among these studies are not well understood; however, the authors concluded that the severity of these changes was minimal. Taken together, the present findings show that short SWCNT exposure induced granulomatous inflammation in the lungs as a foreign-body reaction, whereas macrophage-containing granulomas neighboring MWCNT-aggregation sites and cell debris were not found during the observation period. We suggest that different types of inflammatory responses are elicited by short SWCNTs and MWCNTs, based on histopathological findings.

Third, DNA-microarray results revealed differing mRNA-expression patterns of individual representative genes that were associated with responses to stimuli between rats administered SWCNTs or MWCNTs instillations. Previously, we examined gene-expression profiles of lung tissues intratracheally instilled with ultrafine nickel oxides or C60 fullerenes, and the results suggested that gene-expression profile analysis can provide valuable information regarding the effects of nanomaterials (Fujita et al., 2009; Fujita et al., 2010). Several genes involved in "response to stimulus" [GO: 0050896] were upregulated as potential lung-tissue biomarkers after impurity-free SWCNT instillation (Fujita et al., 2015a). In this study, expression levels of the *Ccl2, Ccl7, Ccl9, Ccl12, Mmp7, Mmp12,* and *Spp1* genes increased during the observation period, except at 30 days post-instillation exposure in SW-H group. In contrast, expression of the *Ccl2, Ccl7, Ccl12, Mmp7,* and *Spp1* genes were markedly upregulated at 1 or 3 days post-instillation exposure, after which they decreased over time for up to 90 days post-instillation exposure in the MW-H group.

By integrating the BALF analysis data, histopathological findings, and transcriptional profiling data, we conclude that short SWCNTs facilitate persistent pulmonary inflammation. Further, short MWCNTs might directly impact the alveolar space immediately after the instillation. However, pulmonary inflammation decreased in a time-dependent manner.

While no large differences were found in the cell counts in PCLFs from the SWCNT-exposed group during the observation period, the total nucleated cells and macrophage counts in PCLFs from the MWCNT-exposed group significantly increased at 30 and 90 days post-instillation exposure. High total protein levels were found at 90 days post-instillation exposure in the MW-H-exposed groups. IL-18 and SPP1 levels in the MW-H groups significantly increased compared to those of the vehicle control groups at 30 and 90 days post-instillation exposure. We suggest that short SWCNT instillation induced low levels of pleural inflammation and that short MWCNT instillation time-dependently induced pleural inflammation. Murphy et al. proposed that CNT clearance from the pleural space occurs in a length-dependent manner (Murphy et al., 2011). Short fibers and small CNT tangles can deposit in the alveoli, locate subpleurally, migrate into the pleural space, and exit in the pleural fluid through the stomata, where they follow the lymphatic drainage to the mediastinal lymph nodes. While long fibers and

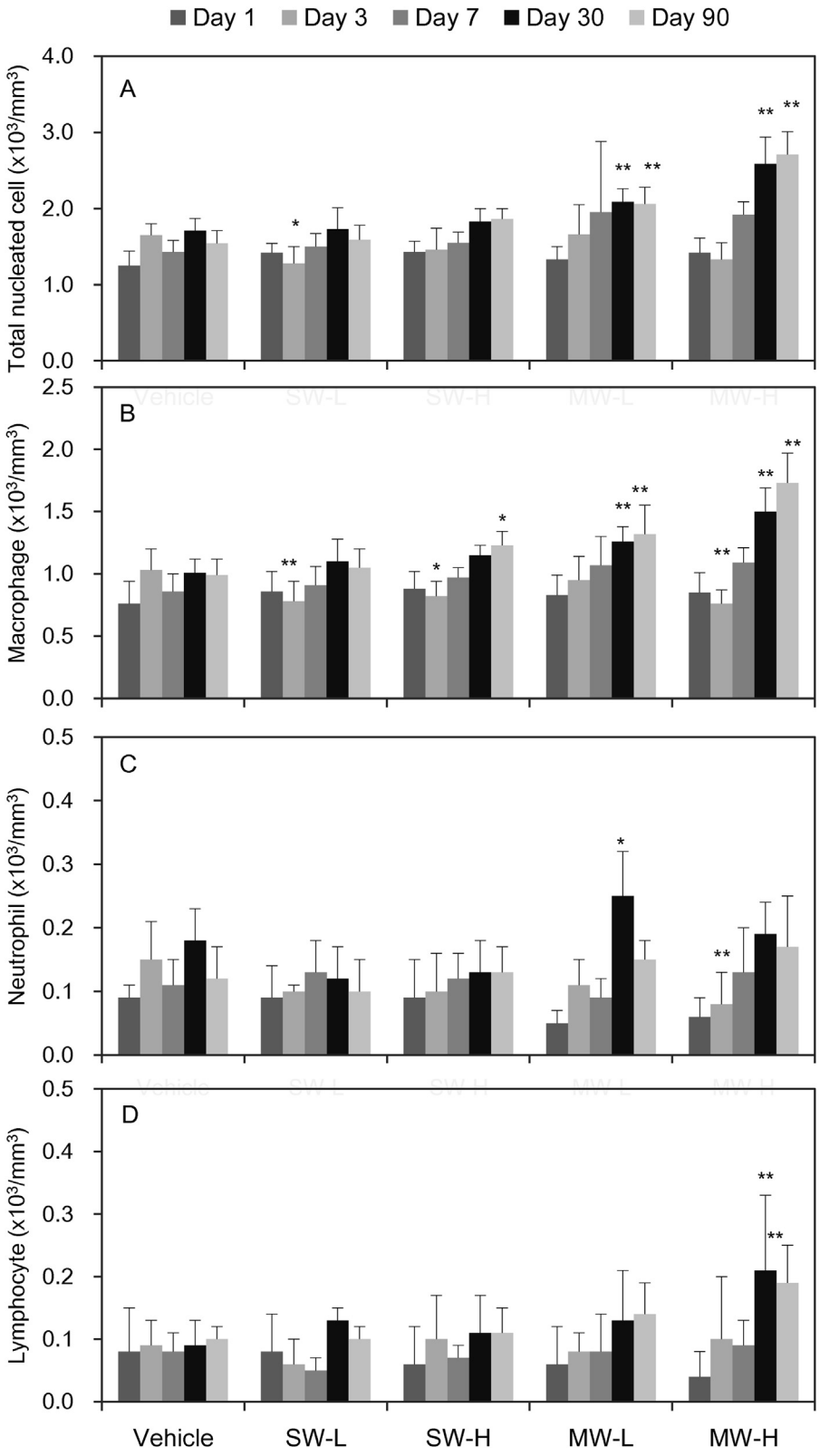


**Fig. 7.** Total nucleated cells (A), macrophages (B), neutrophils (C), and lymphocytes (D) in PCLFs following exposure of rats to vehicle controls, SWCNTs (SW-L or SW-H), or MWCNTs (MW-L or MW-H) at the indicated time points. The resulting values were analyzed by comparing data from the treated and vehicle control groups by Dunnett's procedure based on the re-sampling method ($^{*}p < 0.05$, $^{**}p < 0.01$), after the data were found to be non-homogeneous by Bartlett's test for homogeneity of distribution ($p < 0.20$).

long CNTs also reach the pleural space from subpleural alveoli, they cannot migrate into the stomata and are retained, where they cause inflammation and potential long-term disease (Murphy et al., 2011), based on findings with MWCNTs. The length of short CNTs is approximately 0.5–2.0 μm. In this study, histopathological findings revealed the needle-like MWCNTs pierced into the

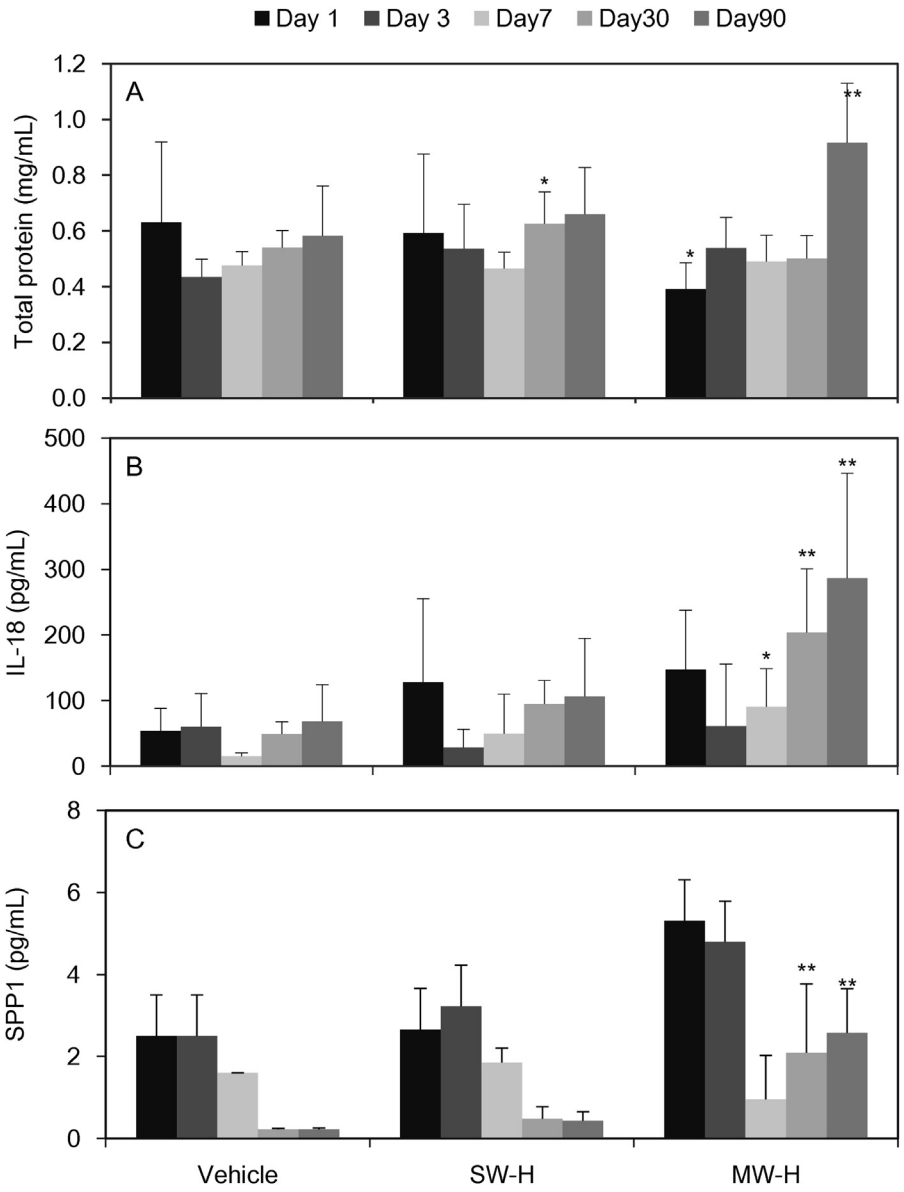


**Fig. 8.** Total protein content (A), IL-18 (B), and SPP1 (C) in PCLFs following the exposure of rats to vehicle controls, SWCNTs (SW-H), or MWCNTs (MW-H) at the indicated time points. The resulting values were analyzed by comparing data from the treated and vehicle control groups by Dunnett's procedure based on the re-sampling method ($^{*}p < 0.05$, $^{**}p < 0.01$), after the data were found to be non-homogeneous by Bartlett's test for homogeneity of distribution ($p < 0.20$).

alveolar wall and alveolar macrophages. We suggest that short MWCNTs reached the visceral pleura and then induced inflammation in the pleural cavity. Alternatively, short MWCNT may flow through the pleural fluid via the stomata after their instillation and then induce inflammation in the pleural space.

Both SWCNTs and MWCNTs were observed in the mediastinal lymph nodes at 90 days post-instillation exposure. MWCNTs, intratracheally instilled in rats, migrated to the posterior mediastinal lymph nodes. MWCNT deposition in these lymph nodes gradually increased in a dose-dependent manner during the post-instillation exposure period, culminating in the formation of small aggregates of MWCNT-laden macrophages on day 91, which could possibly progress to form microgranulomas (Aiso et al., 2011). Interestingly, results from the present study showed that both MWCNTs and SWCNTs followed the lymphatic drainage into the mediastinal lymph nodes after pleural penetration. Therefore, we suggest that short SWCNTs may also flow through the pleural fluid via the stomata after their instillation and induce inflammation in the pleural space. However, inflammation induced in the pleural cavity was less severe compared with that induced by short MWCNTs. We speculate that these results are relevant to differences in the extent of lung inflammation. Short SWCNTs, which substantially accumulated in the lungs, are inefficiently translocated into the pleura and are deposited in the pleural space. Short MWCNTs, which are not fully processed in the lungs, are translocated to the pleural cavity and cause inflammation. The reasons underlying the different behaviors in response to SWCNTs and MWCNTs observed in BALF or PCLF cells remains unclear. However, they may be due to the physicochemical properties of SWCNTs and MWCNTs, such as their length, diameters, and shapes. To test this hypothesis, further quantitative analysis of SWCNT and MWCNTs in tissues is needed.

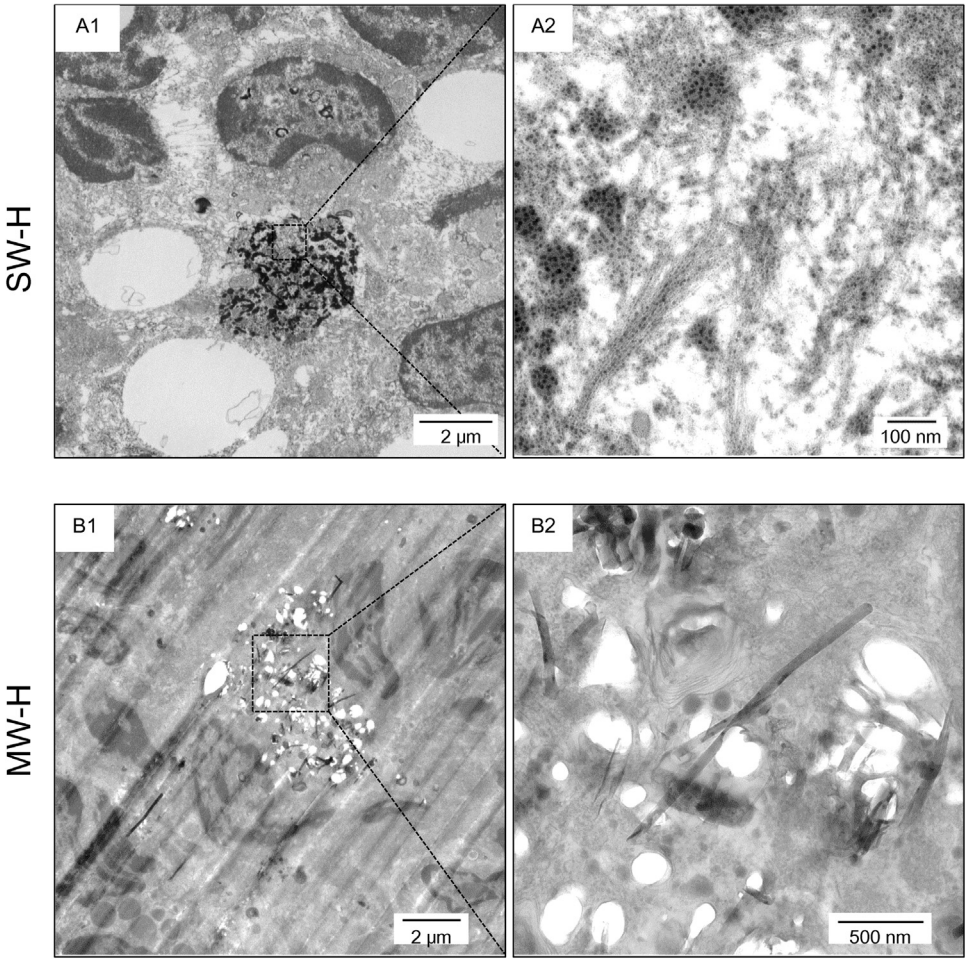


**Fig. 9.** TEM images of SWCNTs or MWCNTs in mediastinal lymph nodes from rats exposed to SW-H or MW-H at 90 days post-instillation. Enlargements of the rectangles for SWCNTs (A1) and MWCNTs (B1) are shown in A2 and B2, respectively.

## 5. Conclusions

The health impacts of CNTs on workers exposed during manufacturing processes may become more serious with increasing developments and use of nanotechnology. Limited research has been conducted to investigate pulmonary and pleural inflammation caused by short CNTs, especially short SWCNTs. The present findings show that short SWCNTs and MWCNTs induce pulmonary and pleural inflammation in different manners and might disperse throughout the whole body after intratracheal instillation. We suggest that the toxicities of short SWCNTs and MWCNTs in respiratory organs should be considered separately. In addition, determining the individual toxicological mechanisms of action of short SWCNTs and MWCNTs, as well as the systemic toxicities of CNTs after inhalation is necessary.

## Conflict of interest

The authors declare that they have no conflicts of interest relevant to this study.

## Acknowledgments

The authors would like to thank Ms. Emiko Kobayashi at the National Institute of Advanced Industrial Science and Technology (AIST) for her assistance in performing the TEM analysis. This study was based on results obtained from a project entitled “Innovative Carbon Nanotubes Composite Materials Project Toward Achieving a Low-Carbon Society (P10024),” which was commissioned by the New Energy and Industrial Technology Development Organization (NEDO) in Japan.

## References

Aiso, S., Kubota, H., Umeda, Y., Kasai, T., Takaya, M., Yamazaki, K., Nagano, K., Sakai, T., Koda, S., Fukushima, S., 2011. Translocation of intratracheally instilled multiwall carbon nanotubes to lung-associated lymph nodes in rats. Ind. Health 49, 215–220.

Beissbarth, T., Speed, T.P., 2004. GOstat: find statistically overrepresented Gene Ontologies within a group of genes. Bioinformatics 20, 1464–1465.

Chou, C.C., Hsiao, H.Y., Hong, Q.S., Chen, C.H., Peng, Y.W., Chen, H.W., Yang, P.C., 2008. Single-walled carbon nanotubes can induce pulmonary injury in mouse model. Nano Lett. 8, 437–445.

Donaldson, K., Aitken, R., Tran, L., Stone, V., Duffin, R., Forrest, G., Alexander, A., 2006. Carbon nanotubes: a review of their properties in relation to pulmonary toxicology and workplace safety. Toxicol. Sci. 92, 5–22.

Donaldson, K., Murphy, F.A., Duffin, R., Poland, C.A., 2010. Asbestos, carbon nanotubes and the pleural mesothelium: a review of the hypothesis regarding the role of long fibre retention in the parietal pleura, inflammation and mesothelioma. Part. Fibre Toxicol. 7, 5.

Donaldson, K., Poland, C.A., Murphy, F.A., MacFarlane, M., Chernova, T., Schinwald, A., 2013. Pulmonary toxicity of carbon nanotubes and asbestos—similarities and differences. Adv. Drug Deliv. Rev. 65, 2078–2086.

Fujita, K., Morimoto, Y., Ogami, A., Tanaka, I., Endoh, S., Uchida, K., Tao, H., Akasaka, M., Inada, M., Yamamoto, K., Fukui, H., Hayakawa, M., Horie, M., Saito, Y., Yoshida, Y., Iwahashi, H., Niki, E., Nakanishi, N., 2009. A gene expression profiling approach to study the influence of ultrafine particles on rat lungs. In: Kim, J.Y., Platt, U., Gu, M.B., Iwahashi, H. (Eds.), Atmospheric and Biological Environmental Monitoring. Springer-Verlag GmbH, The Netherlands, pp. 221–229.

Fujita, K., Morimoto, Y., Endoh, S., Uchida, K., Fukui, H., Ogami, A., Tanaka, I., Horie, M., Yoshida, Y., Iwahashi, H., Nakanishi, J., 2010. Identification of potential biomarkers from gene expression profiles in rat lungs intratracheally instilled with C(60) fullerenes. Toxicology 274, 34–41.

Fujita, K., Endoh, S., Maru, J., Kato, H., Nakamura, A., Kinugasa, S., Shinohara, N., Uchino, K., Fukuda, M., Obara, S., Ema, M., and Hashimoto, H., 2014. Sample preparation and characterization for safety testing of carbon nanotubes, and in vitro cell-based assay. Available at: http://en.aist-riss.jp/assessment/2571/ (accessed 31.03.14.).

Fujita, K., Fukuda, M., Fukui, H., Horie, M., Endoh, S., Uchida, K., Shichiri, M., Morimoto, Y., Ogami, A., Iwahashi, H., 2015a. Intratracheal instillation of single-wall carbon nanotubes in the rat lung induces time-dependent changes in gene expression. Nanotoxicology 9, 290–301.

Fujita, K., Fukuda, M., Endoh, S., Maru, J., Kato, H., Nakamura, A., Shinohara, N., Uchino, K., Honda, K., 2015b. Size effects of single-walled carbon nanotubes on *in vivo* and *in vitro* pulmonary toxicity. Inhal. Toxicol. 27, 207–223.

Kobayashi, N., Naya, M., Ema, M., Endoh, S., Maru, J., Mizuno, K., Nakanishi, J., 2010. Biological response and morphological assessment of individually dispersed multi-wall carbon nanotubes in the lung after intratracheal instillation in rats. Toxicology 276, 143–153.

Lam, C.W., James, J.T., McCluskey, R., Hunter, R.L., 2004. Pulmonary toxicity of single-wall carbon nanotubes in mice 7 and 90 days after intratracheal instillation. Toxicol. Sci. 77, 126–134.

Mühlfeld, C., Poland, C.A., Duffin, R., Brandenberger, C., Murphy, F.A., Rothen-Rutishauser, B., Gehr, P., Donaldson, K., 2012. Differential effects of long and short carbon nanotubes on the gas-exchange region of the mouse lung. Nanotoxicology 6, 867–879.

Ma-Hock, L., Treumann, S., Strauss, V., Brill, S., Luizi, F., Mertler, M., Wiench, K., Gamer, A.O., van Ravenzwaay, B., Landsiedel, R., 2009. Inhalation toxicity of multiwall carbon nanotubes in rats exposed for 3 months. Toxicol. Sci. 112, 468–481.

Morimoto, Y., Hirohashi, M., Horie, M., Ogami, A., Oyabu, T., Myojo, T., Hashiba, M., Mizuguchi, Y., Kambara, T., Lee, B.W., Kuroda, E., Yamamoto, K., Kobayashi, N., Endoh, S., Uchida, K., Nakazato, T., Fujita, K., Nakanishi, J., Tanaka, I., 2012a. Pulmonary toxicity of well-dispersed single-wall carbon nanotubes following intratracheal instillation. J. Nano Res. 18–19, 9–25.

Morimoto, Y., Hirohashi, M., Ogami, A., Oyabu, T., Myojo, T., Todoroki, M., Yamamoto, M., Hashiba, M., Mizuguchi, Y., Lee, B.W., Kuroda, E., Shimada, M., Wang, W.N., Yamamoto, K., Fujita, K., Endoh, S., Uchida, K., Kobayashi, N., Mizuno, K., Inada, M., Tao, H., Nakazato, T., Nakanishi, J., Tanaka, I., 2012b. Pulmonary toxicity of well-dispersed multi-wall carbon nanotubes following inhalation and intratracheal instillation. Nanotoxicology 6, 587–599.

Muller, J., Huaux, F., Moreau, N., Misson, P., Heilier, J.F., Delos, M., Arras, M., Fonseca, A., Nagy, J.B., Lison, D., 2005. Respiratory toxicity of multi-wall carbon nanotubes. Toxicol. Appl. Pharmacol. 207, 221–231.

Murphy, F.A., Poland, C.A., Duffin, R., Al-Jamal, K.T., Ali-Boucetta, H., Nunes, A., Byrne, F., Prina-Mello, A., Volkov, Y., Li, S., Mather, S.J., Bianco, A., Prato, M., MacNee, W., Wallace, W.A., Kostarelos, K., Donaldson, K., 2011. Length-dependent retention of carbon nanotubes in the pleural space of mice initiates sustained inflammation and progressive fibrosis on the parietal pleura. Am. J. Pathol. 178, 2587–2600.

Pauluhn, J., 2010. Subchronic 13-week inhalation exposure of rats to multiwalled carbon nanotubes: toxic effects are determined by density of agglomerate structures, not fibrillar structures. Toxicol. Sci. 113, 226–242.

Poland, C.A., Duffin, R., Kinloch, I., Maynard, A., Wallace, W.A., Seaton, A., Stone, V., Brown, S., Macnee, W., Donaldson, K., 2008. Carbon nanotubes introduced into the abdominal cavity of mice show asbestos-like pathogenicity in a pilot study. Nat. Nanotechnol. 3, 423–428.

Porter, D.W., Hubbs, A.F., Mercer, R.R., Wu, N., Wolfarth, M.G., Sriram, K., Leonard, S., Battelli, L., Schwegler-Berry, D., Friend, S., Andrew, M., Chen, B.T., Tsuruoka, S., Endo, M., Castranova, V., 2010. Mouse pulmonary dose- and time course-responses induced by exposure to multi-walled carbon nanotubes. Toxicology 269, 136–147.

Porter, D.W., Hubbs, A.F., Chen, B.T., McKinney, W., Mercer, R.R., Wolfarth, M.G., Battelli, L., Wu, N., Sriram, K., Leonard, S., Andrew, M., Willard, P., Tsuruoka, S., Endo, M., Tsukada, T., Munekane, F., Frazer, D.G., Castranova, V., 2013. Acute pulmonary dose-responses to inhaled multi-walled carbon nanotubes. Nanotoxicology 7, 1179–1194.

Ryman-Rasmussen, J.P., Cesta, M.F., Brody, A.R., Shipley-Phillips, J.K., Everitt, J.I., Tewksbury, E.W., Moss, O.R., Wong, B.A., Dodd, D.E., Andersen, M.E., Bonner, J.C., 2009. Inhaled carbon nanotubes reach the subpleural tissue in mice. Nat. Nanotechnol. 4, 747–751.

Shvedova, A.A., Yanamala, N., Kisin, E.R., Tkach, A.V., Murray, A.R., Hubbs, A., Chirila, M.M., Keohavong, P., Sycheva, L.P., Kagan, V.E., Castranova, V., 2014. Long-term effects of carbon containing engineered nanomaterials and asbestos in the lung: one year postexposure comparisons. Am. J. Physiol. Lung Cell Mol. Physiol. 306, L170–L182.

Xu, J., Futakuchi, M., Shimizu, H., Alexander, D.B., Yanagihara, K., Fukamachi, K., Suzui, M., Kanno, J., Hirose, A., Ogata, A., Sakamoto, Y., Nakae, D., Omori, T., Tsuda, H., 2012. Multi-walled carbon nanotubes translocate into the pleural cavity and induce visceral mesothelial proliferation in rats. Cancer Sci. 103, 2045–2050.

Xu, J., Alexander, D.B., Futakuchi, M., Numano, T., Fukamachi, K., Suzui, M., Omori, T., Kanno, J., Hirose, A., Tsuda, H., 2014. Size- and shape-dependent pleural translocation deposition, fibrogenesis, and mesothelial proliferation by multiwalled carbon nanotubes. Cancer Sci. 105, 763–769.

Warheit, D.B., Laurence, B.R., Reed, K.L., Roach, D.H., Reynolds, G.A., Webb, T.R., 2004. Comparative pulmonary toxicity assessment of single-wall carbon nanotubes in rats. Toxicol. Sci. 77, 117–125.